ORIGINAL ARTICLE

http://dx.doi.org/10.1590/S2675-28242020068314

OCEAN AND COASTAL RESEARCH

Tidal inlet migration and formation: the case of the Ararapira inlet – Brazil

Diana Italiani[1*], Eduardo Siegle[2], Mauricio Almeida Noernberg[1]

[1] Centro de Estudos do Mar- UFPR, PGSISCO - Av. Beira-mar, s/n - P.O.Box: 61 - Pontal do Paraná- 83255-976 - PR - Brazil
[2] Instituto Oceanográfico - USP, Departamento de Oceanografia Física, Química e Geológica - São Paulo - Praça do Oceanográfico, 191 - Cidade Universitária - Butantã - 05508-120 - SP - Brazil

*Corresponding author: dianajgd@gmail.com

ABSTRACT

The aim of this study is to assess the morphological evolution of the Ararapira (Brazil) barrier-inlet system, at different time scales. Based on satellite imagery, elevation data, and *in-situ* observations, we quantify the morphological evolution of the region. Results show that the Ararapira inlet migrated continuously southwards, moving updrift, with erosion at its southern margin and intercalated erosion and accretion at the northern margin. At approximately 5.5 km north of the old inlet, the gradual narrowing of the sandy barrier due to channel meandering and coastal erosion resulted in its breaching, in August 2018. We document the initial stages of the new inlet, which after opening, presents intense erosion at its southern margin, resulting in the channel widening to ~1 km. After the barrier breaches, the system begins to adjust to a new equilibrium condition, with the widening of the new inlet being balanced by the gradual closure of the old inlet. These drastic environmental changes control the functioning of such systems, and our results provide important background information for their use and management.

Descriptors: Tidal inlet processes, Spit breaching, Coastline trends.

INTRODUCTION

Coastline variation occurs in various time scales affecting human life in coastal areas, especially in the decadal scale. Coastal erosion and deposition phenomena associated with inlet migration depend on the geological configuration, the sediment processes sources and sink and the action of waves, tide, and currents (Dean and Dalrymple, 2002).

Generally, the formation of tidal inlets requires the presence of an embayment and the development of barriers. In coastal plain configurations, the embayment or back-barrier is usually created through the barrier islands' formation. In some instances, the establishment of this embayment occurred due to sea-level rise by flooding an irregular coastal limit during the Holocene (Davis Jr. and Fitzgerald, 2004). Due to its significant influence on shoreline variation, tidal inlets focus on the most dynamic changes that occur along barrier island coasts, with its morphology being the result of their adjustment to the effective action of both tidal currents and waves (Hayes and Fitzgerald, 2013).

Wave-generated currents rework and transport coastal sediments, with the intensity of these processes depending on the energy and direction of the waves approaching the coast. Under constant energy conditions, the maximum capacity of sediment

Submitted on: 6/March/2020
Approved on: 18/June/2020
Associate Editor: Felipe Toledo

Editor: Rubens M. Lopes

transport occurs when waves approach a shoreline at an angle of 45° when increasing or decreasing. This angle makes the flow capacity alongshore decrease, which allows establishing a relative quantification of the coastal drift (Siegle and Asp, 2007). However, the presence of inlets and its adjacent features can partially interrupt the longshore transport, affecting the sand supply; consequently, the erosion and deposition patterns on nearby beaches (Fitzgerald, 1988). Studies determine the direction of the longshore transport focus on morphological features, like spits, tidal deltas, sand shoals, and their evolution in space and time. In general, river mouths and lagoon inlets migrate downdrift, developing a spit that grows in the longshore drift direction (Komar, 1998; Vila-Concejo et al., 2003; FitzGerald, 1988; Tessler and Mahiques, 1993; Souza, 1999; Cassiano and Siegle, 2010; Cussioli et al., 2011). However, in some specific cases, inlets migrate in the opposite direction of the dominant longshore drift (e.g., Aubrey and Speer, 1984), which is the case of the Ararapira inlet, a fact already pointed out by Tessler and Mahiques (1993) and subject of our study. The inlet migrates southwards, opposing the dominant northwards longshore drift (Trombetta et al., 2018; Silva et al., 2016).

In some cases, a major back-barrier tidal channel approaches the inlet at an oblique angle, and the ebb-tidal currents flow toward the margin of the inlet throat. The inlet will migrate in the direction of the flow, even if the margin is the updrift side of the main channel. A similar process occurs in a river where strong currents are focused along the outside of a meander bend, causing erosion and channel migration (Aubrey and Speer, 1984). Updrift migrating inlets, in general, are found along coasts with small to moderate net sand longshore transport rates (Davis Jr. and Fitzgerald, 2004). When ebb and flood flows are well balanced, the longshore sand supply is abundant, and the estuary channel is normal to the inlet, the estuary may fill with sands derived from updrift sources, as the flood tidal delta growth accompanies the migration of the inlet (Aubrey and Speer, 1984).

Inlet formation by the breaching of a narrow section in a barrier shoreline is typical in coastal lagoons. Once there is an opening to the back-barrier, and if there are sufficient tidal forces to create an ebb and flood flow through the breach, it may be permanent after the storm surge subsides (Liu et al., 1993). The formation of new inlets within barriers islands during extreme storms is of particular interest as the sediment-transport processes are extremely active, leading to the rapid evolution of the inlet morphology (Komar, 1996).

For long inlet channels, the exchange of water between the ocean and the back-barrier channel or bay is retarded, leading to significant water-level differences between the ocean and bay. Such processes make the barrier highly susceptible to breaching, particularly during storms. With the formation of a new inlet in a hydraulically more favorable position, the tidal prism is diverted to the new inlet, and the old inlet tends to close (Davies Jr. and Fitzgerald, 2004).

Observing the shoreline variation at different periods of the year is a fundamental task for coastal monitoring. It can offer an essential contribution to the protection and sustainable development of the coastal zone (Alesheikh et al., 2007). The use of remote sensing for this purpose is advantageous because it allows a broader observation capacity of the system compared to in situ data acquisition methods and continuous registers.

This study assesses the morphology of the Ararapira Inlet system at two different time scales based on satellite imagery and *in situ* topographic data: i. decadal evolution of the updrift migrating inlet; and ii. the recent breaching of the barrier creating a new inlet (August 28, 2018).

STUDY AREA

The Ararapira Inlet is located on the coastal border between Paraná and São Paulo States, southeast Brazil, inserted in the Cananeia-Paranaguá estuarine-lagoon Complex. The Ararapira channel is an SSW-NNE elongated and meandering water body with its main channel running along the coast, separated from the ocean by Cardoso Island. It extends for approximately 16 km and has an average width and depth of 400 m and 5 m. It communicates with the Trapandé Bay (Cananeia) on its northernmost part through the Ararapira Channel and with the Pinheiros Bay to the South, through the Varadouro Channel, an artificial channel excavated in the 1950s (Fig.1).

The Barra do Ararapira Village is located at the western margin of the channel, close to its inlet,

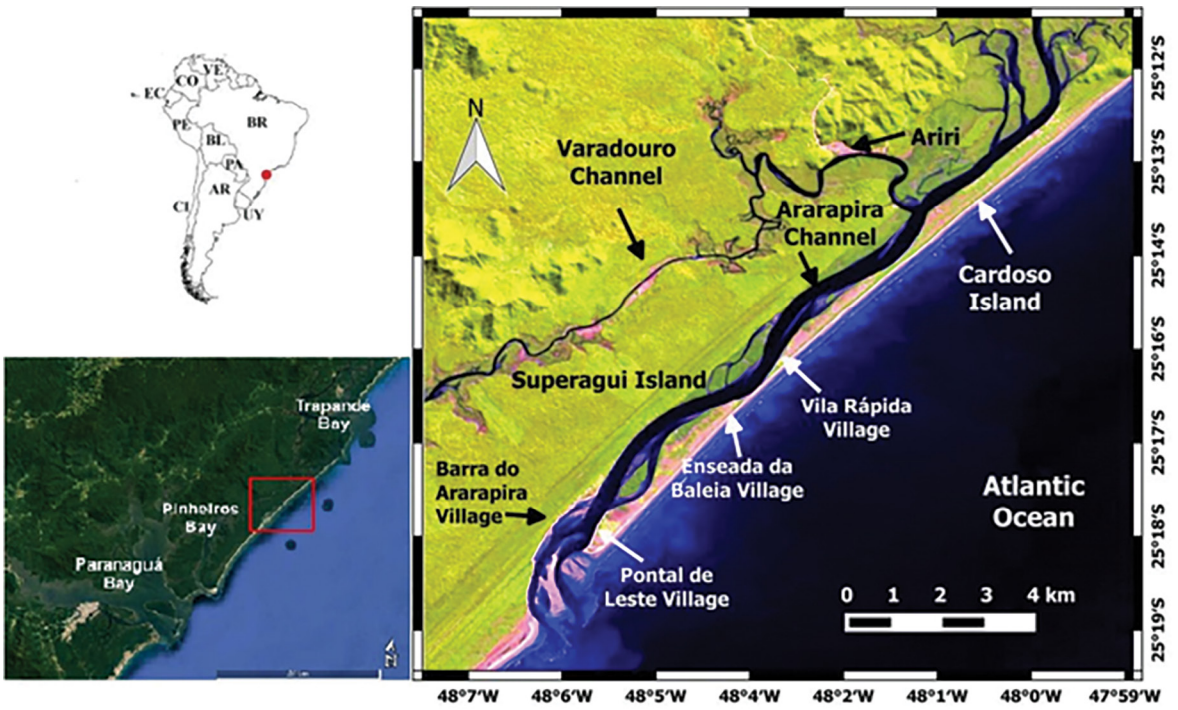

Figure 1. Location of the study area in Southeast Brazil, indicating its main features (Images: Google Earth and Land, Sat. 8-5/14/2017).

with dominant erosive processes; at the opposite margin is the Pontal de Leste Village. Further north, close to the barrier island's narrowest portion, are the communities of Enseada da Baleia and Vila Rápida.

The Ararapira Inlet had a 2 km (2016) wide channel separating Superagüi Island from Cardoso Island. It is filled with tidal delta deposits dominated by wave and flood tide features (Angulo et al., 2009). The estuary channel is separated from the ocean by an 18 km long and narrow spit (varying between 20 and 800 m in width), extending SW from Cardoso Island (Müller, 2010). According to Angulo et al. (2007), the spit has been formed by lateral southward migration in the last 700 to 1100 years.

Prevailing winds from eastern and southern quadrants influence the region, a consequence of the passage of extratropical cyclones (Rocha et al., 2004), and the presence of Tropical Anticyclones of the South Atlantic (ATAS) which is responsible for the winds from NE to E with constant frequency acting between 10 and 40 degrees of latitude (Tessler and Goya, 2005). The precipitation regime presents an annual mean of around 2500 mm. The prevailing wave direction, with higher sediment transport capacity, varies between S, SSE and SE quadrants (Portobrás, 1983; Pianca et al., 2010; Nemes and Marone, 2013; Silva et al., 2016; Ambrosio et al., 2020), with dominant wave height being 1.5 m and period of 8 s (Silva et al., 2016). Waves generated longshore drift in the region presents a net northwards drift. However, presenting seasonal variations with southwards drift during summer and spring months, as observed by Silva et al. (2016) for the Ilha Comprida area, with similar coastline orientation at around 50 km to the north of the Ararapira inlet. The region is subjected to a semi-diurnal microtidal regime, with the spring tidal range of about 1.2 m and a neap tidal range of about 0.25 m (Harari and Camargo, 1994). Meteorological tides are also frequent and can add up to 0.8 m above mean sea level (Marone and Camargo, 1995). The channels that form the Cardoso island and the Ararapira inlet are connections to the Cananeia estuary (to the north) and the Paranaguá bay (to the South). The channels that form the system are tidal channels that receive only small freshwater contributions. Salinity in the main channel is around 30, and in the connecting channel (Ariri), it varies between 5 and 25 throughout the tidal cycle (Italiani, 2019).

The sediments of the Ararapira Channel are composed of fine sand in the southern sector, with

less river contribution (Angulo et al., 2019). In central and northern sectors, sediment is composed of silt and clay, corresponding to the channel's confined areas, associated with shoals, narrow tide channel, and inlets of small rivers located on both margins of the channel (Kumpera, 2007).

METHODS

To assess the long- (decades) and short-term (months) evolution of the Ararapira barrier-inlet system, we combine satellite images and *in situ* morphological surveys. Using plan-view coastline changes, based on satellite images and digital elevation models and profiles, we could quantify the morphological evolution of the system based on surveys.

Long-term assessment

The assessment of the shoreline variation and estimates of erosion rates from 1985 to 2016, in a frequency of approximately five years, was done by using six Landsat 5 (1985/05/06, 1991/05/23, 1996/04/02, 2001/05/18, 2006/09/05, 2011/08/02) and one Landsat 8 (2016) images downloaded from the National Institute of Space Research (INPE) database. All the images were registered to the WGS-84 Datum using the Landsat 8 2016/12/05 scene as a reference with errors less than 1 pixel. Images have been georeferenced through 18 spatially distributed ground control points used with a two-order polynomial geometrical model and a bilinear interpolation method. The Normalized Difference Water Index (NDWI) presented by McFeeters (1996) was used to contrast the shoreline features, and a threshold of separation between land and water was defined.

The morphological variation of the inlet and the narrowest portion of the Cardoso Island spit (Enseada da Baleia) was estimated using five Landsat 7 (1999-2003) and four Landsat 8 (2015-2018) images. For all dates, the panchromatic band (15 m resolution) and multispectral bands (30 m: RGB bands 5, 4, and 3) were merged using Superimpose and Pansharpening tools available in the software QGIS Desktop. Afterward, the Landsat 7 images were registered using the Landsat 8 (2015) image as a reference, with errors of less than 1 pixel. The inlet subaerial areas were calculated (Superagüi margin, tidal delta, and Pontal de Leste margin) to estimate the morphological variation. The areas for both margins were determined from the edge of the vegetation as the limit of the emerged part, considering 2017 as a reference.

Short-term assessment

Two topographic surveys of the inlet and adjacent areas were performed on March 2017 and on September 2018 with a post-processed kinematic method using a Differential Global Positioning System (DGPS); providing latitude, longitude and ellipsoidal height data obtained from a mobile receiver with vertical and horizontal precision of ± 5 cm. Two Leica Viva CS15 instruments were used: a fixed base stationed at Cardoso Island (north) and the other a mobile rover. Data processing was performed using the Leica Geo Office (LGO) software, where the base was post-processed by triangulation with data from Cananeia and Curitiba bases from the Brazilian Network of Continuous Monitoring GNSS (RBMC) available at www.ibge.gov.br. Ellipsoidal heights (h) were converted to orthometric heights (H) from the value of the geoidal height (N) provided by geoidal curling, obtained by the geoidal model (MAPGEO2015), also from IBGE, calculated as H=h-N.

The bathymetric survey of the new inlet was conducted using a Garmin EchoMap CHIRP 42dv installed on a vessel with a Leica mobile receiver working on the DGPS system. The onboard setup fills the requirements for bathymetric surveys defined by the Brazilian Navy, providing horizontal precision of ± 5 cm and vertical precision of about ± 10 cm. The depth values were obtained using the method developed by Ferreira et al. (2014), eliminating the need for tidal correction.

For the sites where topographic data were collected twice (2017/03 and 2018/09), the variation of the orthometric height and the sediment volume was estimated through grid data differences from the digital terrain models obtained through interpolation using the Kriging method. Comparatively, this interpolation method has presented the best results for the interpolated grid when comparing interpolated results to measured profiles. The panchromatic band from CEBERS-4 image (5m resolution), acquired in September 2018, was used to analyze the new inlet shoreline variation.

RESULTS

The results show the morphologic evolution of the Ararapira inlet at different time scales, including the recent evolution of the newly formed inlet. The migration of the old Ararapira inlet is evaluated on a ten-year time scale. The formation and evolution of the new inlet are analyzed on shorter time scales following its recent evolution after the barrier was broken in August 2018.

Ararapira Inlet (old inlet)

The coastline analysis of the old Ararapira inlet is based on the evolution of the system's different features, such as the spit that forms the northern margin of the inlet, the southern margin of the inlet, and the distance between both, giving the channel width. The coastline evolution between 1985 and 2016 revealed a continuous southward growth of the spit (Fig. 2a, 2b, 2c), following the updrift migration of the inlet. The southernmost position of the spit was reached in 2006, with a southward spit growth of around 700 m (Fig. 2d), followed by a 115 m retraction in 2011 (Fig. 2e), and further eroding northwards by 350 m until 2016 (Fig. 2e).

The inlet channel width increased by approximately 1300 m between 1985 and 2016 (Fig. 3) due to erosion processes occurring at both margins. However, higher and more constant erosion rates were observed at its southern margin due to the continuous updrift migration of the inlet.

New topographic profiles of the two inlet margins show differences between them regarding the actual erosion processes (Fig. 4). The southern margin profile presents a steeper slope and higher elevation, features observed in erosive margins. On the other side, the growing northern margin presents a flatter profile and low elevations, easily flooded during high tides.

The main inlet channel is divided by a large sandbar that is part of the tidal delta formed by sediment being transported alongshore into the inlet. In the inner portion of the channel, where the sandbars are protected from wave action, they are better developed and are exposed during low tides. Much of the sediment eroded from both margins may be transported to the ebb-tidal delta.

At the inner portion of the southern margin of the Ararapira inlet, it is possible to observe continuous erosive processes, while at the oceanward margin, accretion is observed (Fig. 5). However, erosive rates at the inner margin are always higher than accretion rates on the adjacent beach (Fig.6).

Figure 6 shows the delimitation of the three subaerial areas used to assess the sediment balance in 1999 and 2018. Superagüi, at the southern and eastern margin of the channel, is the sector that lost more area during the period and, in 1999, 2000, 2002, 2003 (Fig. 7), no subaerial delta is visible. However, the total value of the emerging area showed a quasicontinuous oscillation, with a maximum difference of 40 km^2 between all years, except for 2016, which presented lower values than other years.

The southern margin height variation, between April 2017 and September 2018 (Fig. 8), presented a positive volume of 10,815m^3. Values show that the sedimentation processes were concentrated at the inner margin, while erosion happened at the outer margin.

Formation of the new inlet

The width of the narrowest part of the Cardoso Island spit, approximately 6 km north of the old inlet and where the new inlet has been formed, decreased around 160 m between 1985 and 2016 (Fig. 9) in a discontinuous way, alternating between erosion and accretion periods (Fig. 10).

Based on the morphological surveys, some profiles have been defined crossing the narrow part of the Cardoso Island spit, before its breaching (Figure 11). The topographic profiles 3 and 4, in the narrowest part of the spit, present the lowest elevation throughout their extension in the 2017 data (Fig. 11), and the other profiles are well demarcated by dunes features and show that the inner margin of the back-barrier is much steeper than the ocean side. The most significant variation in height difference before and after the opening of the new inlet is in profile 2. After the inlet opening, the survey conducted on September 27, 2018, shows a 4 m deep channel, contrasting with the 5 m high barrier observed in April 2017.

After the opening of the new inlet at August 28, 2018, the morphological evolution of its margins from September 2018 to January 2019 (Fig. 12),

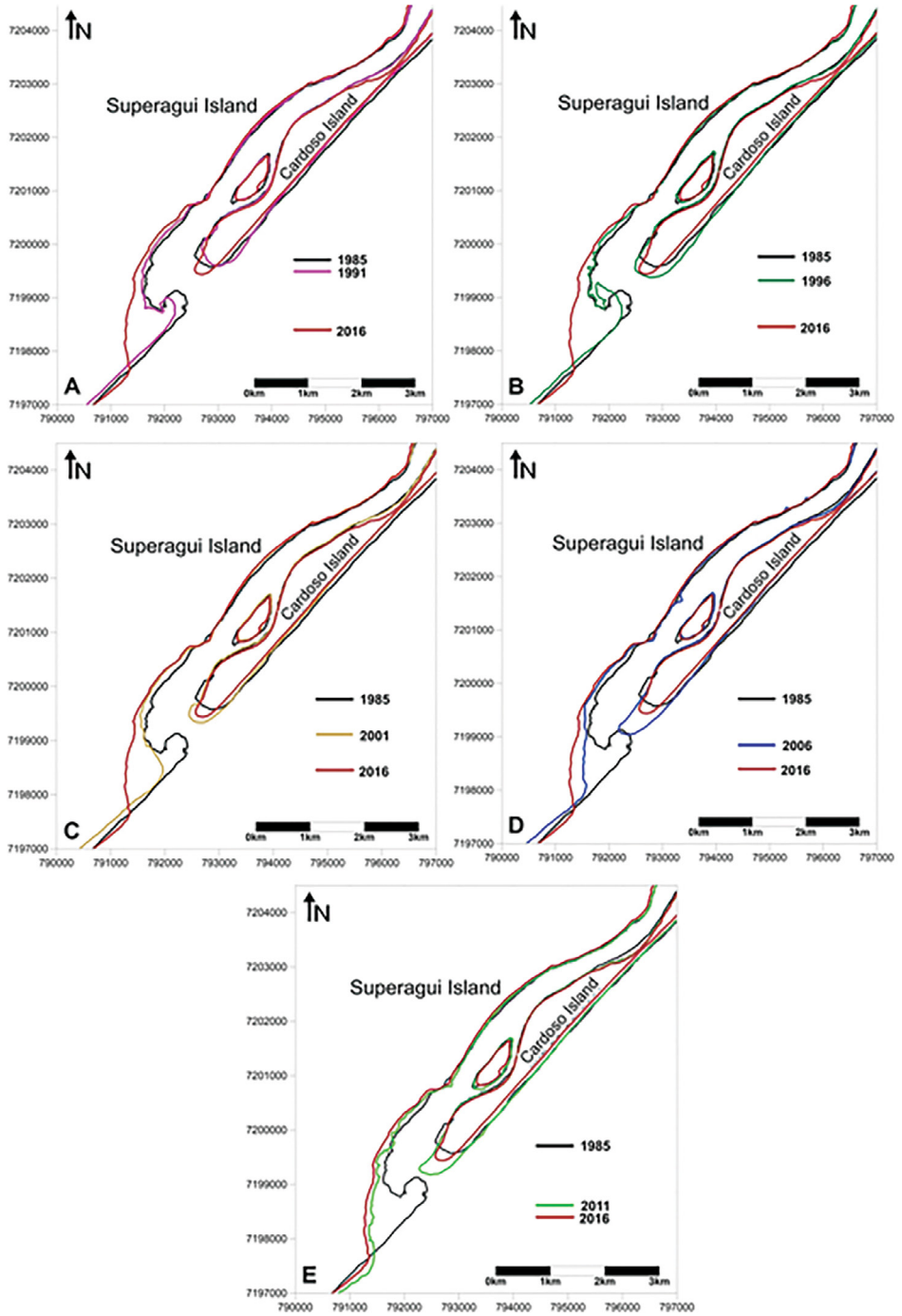

Figure 2. Coastline evolution between 1985 and 2016 based on the available satellite images. Intermediate years are shown in A (1991), B (1996), C (2001), D (2006) and E (2011).

shows a higher rate of erosion at its southern margin, during September 2018, forming the main channel in the south sector of the eroded area. However, from September 2018 to January 2019, it was the northern margin that eroded most, retreating 440 m, while the southern margin eroded 140 m.

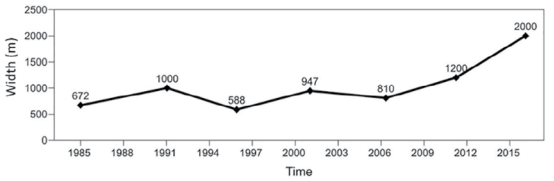

Figure 3. Old Ararapira inlet width variation between 1985 and 2016, based on the available satellite images.

The volume variation in the area where the barrier breach occurred, has been estimated at 251,710 m^3. Considering that by the end of August 2018, the inlet was still closed, almost half of the volume was eroded in less than a month.

DISCUSSION

Results show that while the southern margin of the old inlet suffered a constant process of erosion between 1985 and 2016, the northern margin presented both deposition and erosion processes at around 1 km. These processes widened the old inlet by about 1300 m during the last decades, oscillating until 2006 and growing continuously since then. The inlet widening happened probably due to the formation of another channel through breaching the sand spit that forms the inlet margin. The constant southward migration (updrift) process of the Ararapira Inlet has already been analyzed and discussed in several studies (Tessler, 1988; Angulo, 1993; Tessler and Mahiques, 1993; Angulo, 1999; Mihaly and Angulo, 2002; Muller, 2007; Angulo et al., 2009; Muller, 2010; Bazzo, 2011). According to Angulo (1993), the concave form of the southern margin supports erosive processes governed by ebb currents in a similar process of river meanders. The same process has also been observed by Tessler (1988). Mihaly and Angulo (2002), pointed out the discontinuous erosion and accretion at both margins, showing that these processes could be reversed during short periods according to the oceanographic conditions driving the longshore drift. The Ararapira inlet presents morphological features related to a bending channel forcing updrift migration, similar to Aubrey and Speer (1984) description, with a steep erosive outer bank and an accreting point bar on the inner bank. We can say that the mouth migration, in this case, depends on the orientation of the channel for the coast.

The shoreline variation at the southern margin of the old inlet presented erosion at the inner channel between 1999 and 2018, and accretion on the adjacent beach. This fact can be explained by the hydraulic jetty effect of the ebbing flows acting as a barrier for the northwards longshore drift transport. A reversal in this pattern is observed between 2017 and 2018 with sedimentation in the inner part and erosion in the oceanic margin (Fig.9). Due to the temporal resolution of the available images, it is not clear if this change started before or after the opening of the new inlet. However, with the expected weakening of tidal flows in the old inlet, after the new inlet opening, the meandering effect in the curved channel is weakened, resulting in less erosion of its southern margin. Additionally, the longshore drift is not interrupted with the same strength as before, enabling the bypass of more sediment through the now closing inlet. Despite the continuous decadal process of erosion on the southern margin, the channel width remained virtually constant, indicating the equilibrium of the feature, with erosion in the south being balanced by accretion at the northern margin.

Approximately 5.5 km to the north of the old inlet is the narrow barrier area where the new inlet was formed. According to Mihaly and Angulo (2002), the average barrier width narrowed from 44 m to 36 m during 32 months (from September 1993 to May 1996) and considering constant erosion rates. The barrier was predicted to open in 2012. In a more recent study, Angulo et al. (2009) predicted that it would open between 2012 and 2016. However, the width of the spit of Cardoso Island presented both erosion and accretion processes over the last three decades. Even with the oscillation between the two processes, the barrier width decreased approximately 160 m over the last 30 years. The variable erosion-accretion oscillation (Fig. 11) process explains the uncertainties in the spit breach prediction since these processes depend on the transport mechanisms of coastal sediments related to energetic coastal events associated with meteorological and oceanographic conditions, storm surges and changes in the direction of wave-generated longshore drift currents (e.g., Silva et al., 2016). This area of the barrier has been narrowing due to both, meandering of the inner channel and coastline retreat. Other important

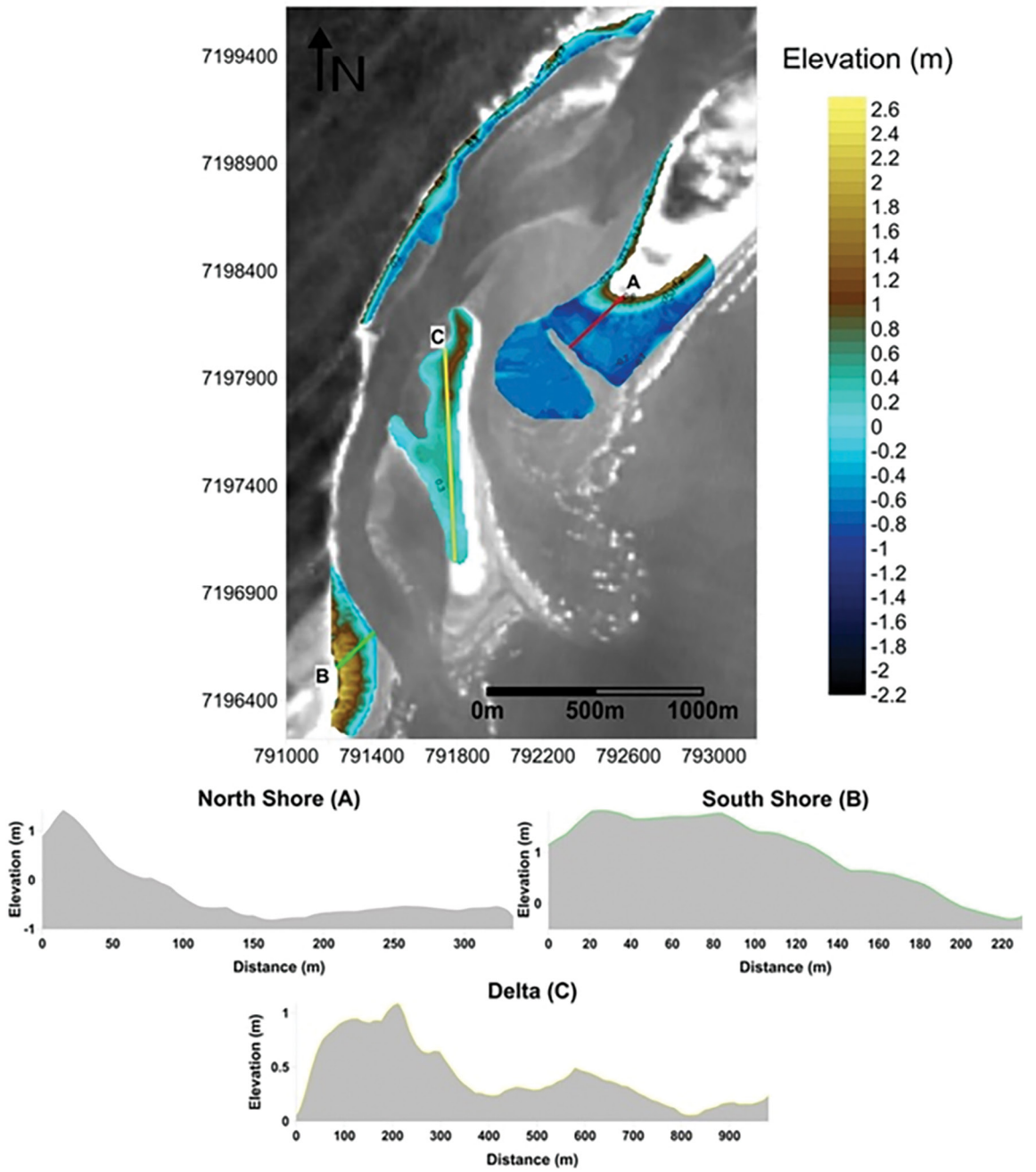

Figure 4. Morphology of the old Ararapira inlet based on topographic surveys (April 2017). Profiles A, B and C represent the morphology of different features of the system.

factors contributing to the acceleration of the erosion process were observed during the fieldwork: aeolian sediment transport from the dunes to the inner channel, especially when the dunes are dry and without vegetation; and pedestrian traffic over the remaining dunes, destroying vegetation and making sediment available for aeolian transport. When possible, trespassing was controlled by local managers through risk area signs and branches blocking the passage.

In October 2016, a storm surge (high-pressure system and southeast winds) associated with spring

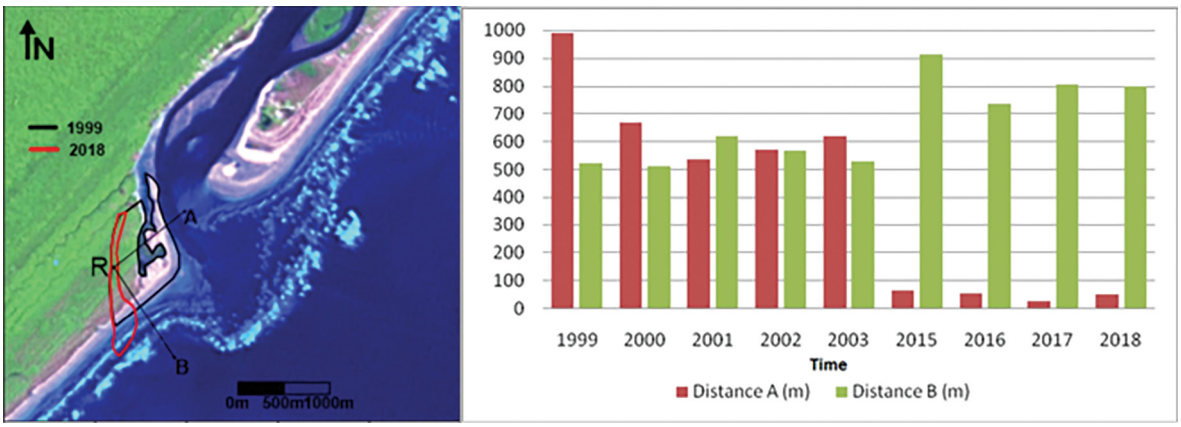

Figure 5. Variation of the area in the southern sector of the Ararapira inlet between 1999 and 2018 based on the coastline extracted from satellite images. Transects A and B are used as a reference in the measurement of the distances from the reference point R to the coastline for each image, as represented in the bar plot (Image: LandSat 7-9/26/1999).

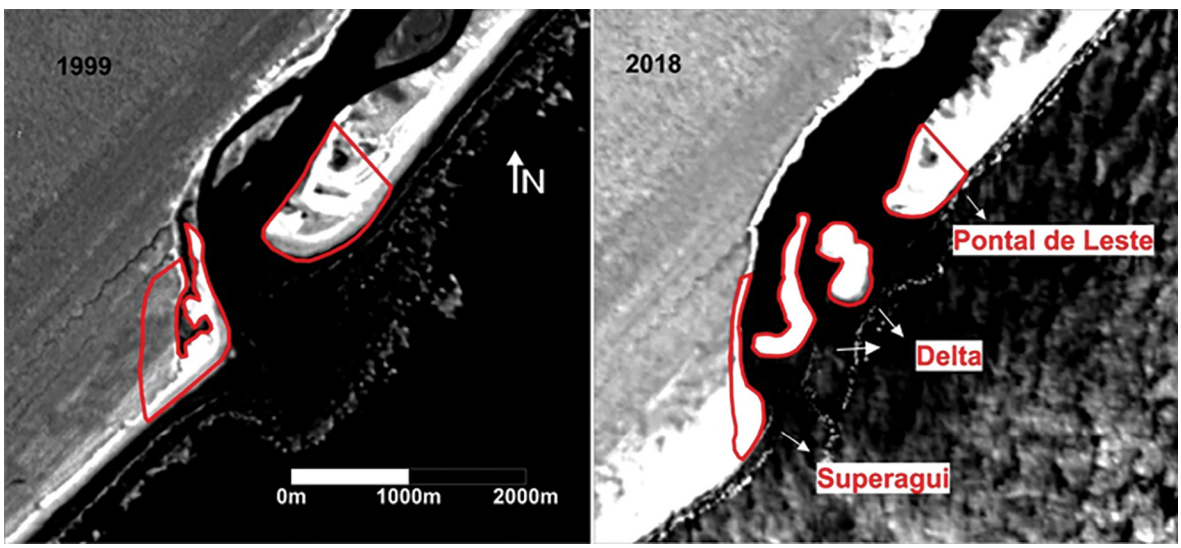

Figure 6. Representation of selected sectors (Superagüi, Delta and Pontal de Leste) of the old Ararapira inlet for 9/26/1999 and 7/20/2018.

tides ended up eroding the Cardoso Island barrier's foredunes. As dunes protect the coastal region from storm surges and extreme tides, and store sediments that are used to replenish beaches during and after storms (Trenhaile, 1997), the foredune erosion resulted in accelerated erosion on the narrowest part of the Cardoso Island in the following years, facilitating overwash processes during extreme events. In August 2018, five frontal systems reached the region. Winds associated with the passage of cold fronts are usually more intense during autumn and winter months (Nimer, 1989), resulting in high energy waves and storm surges in the region (e.g., Pianca et al., 2010). On August 25, the cold front coincided with spring tides and a positive precipitation anomaly of 200 mm in the north of Paraná (CPTEC/INPE). This set of factors contributed to the barrier breach that rapidly evolved to the new inlet.

Four days after opening, the channel was already 170 m wide, according to information provided by the management of the State Park of Cardoso Island. On September 28, the topographic and bathymetric surveys showed it to be 674 m wide. The approximate channel widening rate was 16 m per day, with the transport of sediment of approximately 2 x 105 m^3 during one month, between August and September 2018. From September 28, 2018, to January 28, 2019, the width increased another 576 m, reaching 1250 m

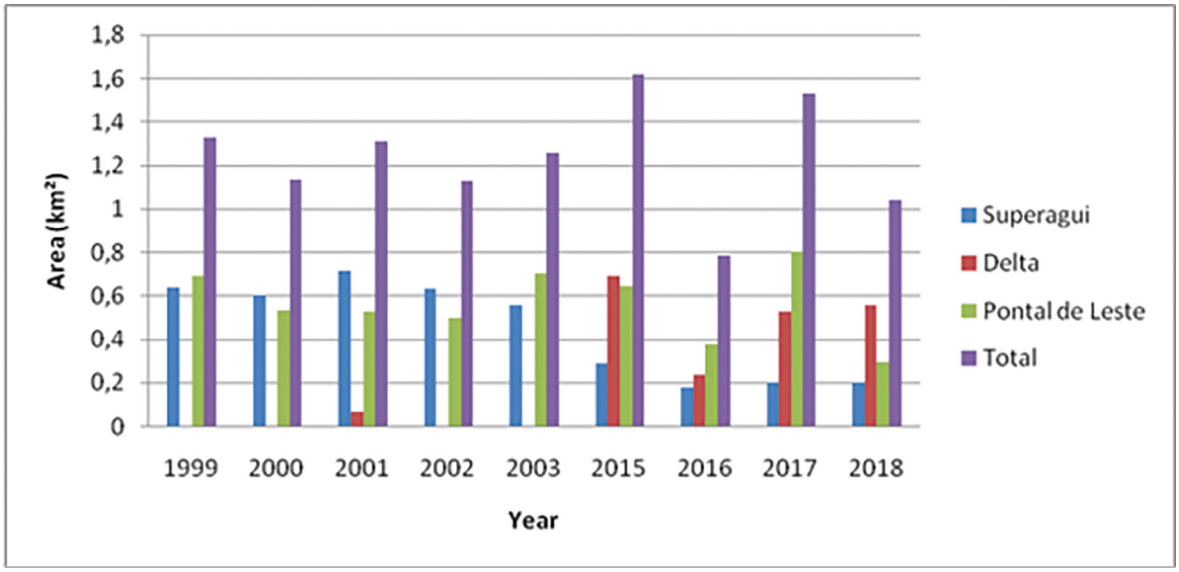

Figure 7. Variation of the subaerial area at three sectors (as defined in Figure 6) of the old Ararapira inlet.

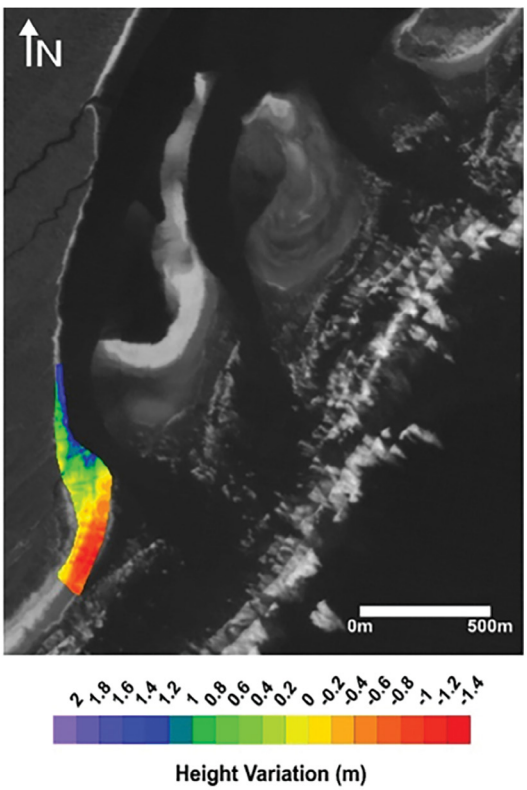

Figure 8. Morphological variation between April 2017 and September 2018 on the southern margin of the old Ararapira inlet, based on topographic surveys.

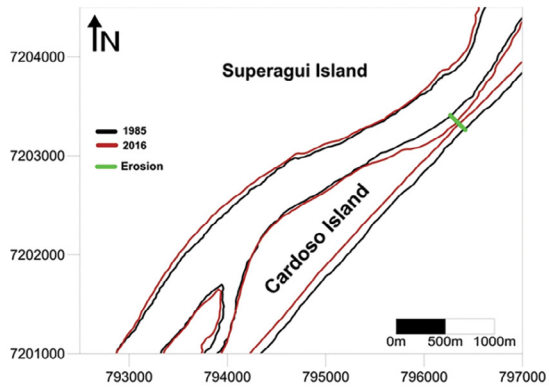

Figure 9. Coastline based on satellite images showing the narrowing of the Cardoso island barrier between 1985 and 2016.

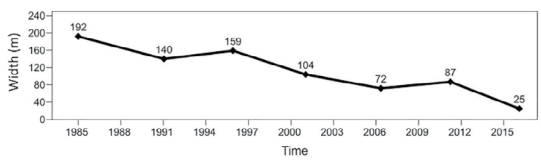

Figure 10. Cardoso Island barrier width variation from 1985 to 2016, based on the available satellite images.

in January 2019. Widening rate has been reduced to 4.8 m per day during this period, followed by even slower rates of about 2.8 m until March 13, 2019, reaching 1370 m (measured from Google Earth Pro Image). This shows that the inlet reaches its expected stabilization, at widths similar to those of the old inlet, beginning to reach its equilibrium cross-sectional area (e.g., O'Brien, 1969; Escoffier, 1940; van de Kreeke, 1992). Storm induced barrier breaching creates connections between lagoons and the ocean

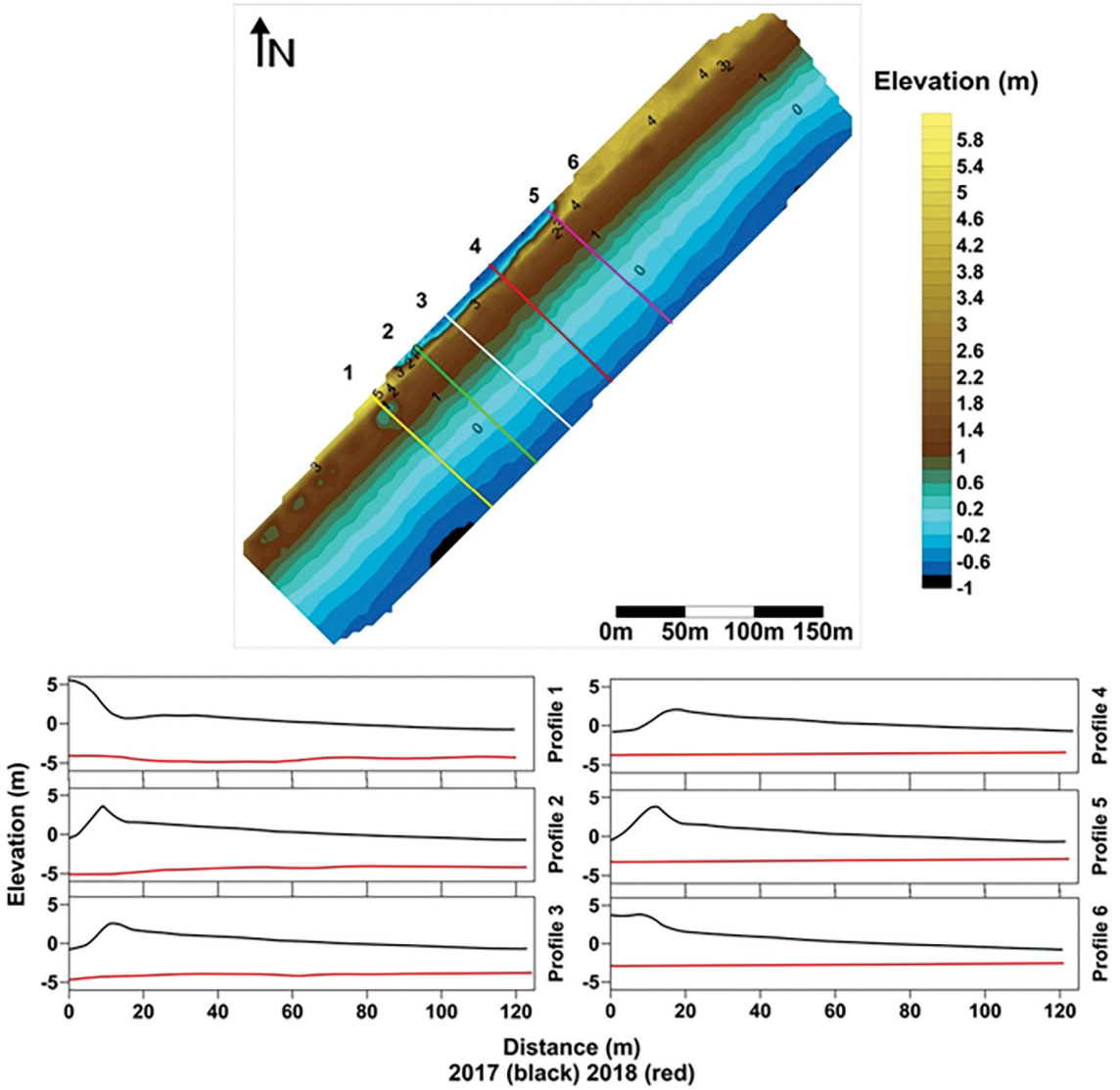

Figure 11. Morphological evolution of the Cardoso Island spit based on topographical surveys from April 2017 (black) and September 2018 (red). Profiles cover the narrowest portion of the spit, as shown in the elevation model. Morphological variations for each profile are shown in the cross-shore profiles.

(Hayes and FitzGerald, 2013; Safak et al., 2016). Once breached, if inlet stabilizing factors, such as tidal currents, dominate over longshore transport (e.g., Escoffier, 1940; Hayes, 1979), the newly formed inlet will remain open and active. These processes control the episodic balance that controls the opening and closure of inlets, for example at Pamlico Sound (Safak et al., 2016), after storms, on idealized coastal barrier models (Reef et al., 2020), or for artificially breached barriers (Moreira et al., 2019).

After the Ararapira new inlet opening, an accelerated erosion process occurred on both margins, although the southern margin presented a higher erosion rate, with the main channel moving southwards during this opening period (Fig. 12). However, in the following months, there is a change in the erosion pattern, with the January 2019 shoreline showing that the northern margin presented a higher erosion rate over time. This alternation of the erosion rate, between the two inlet sides, is usual until the

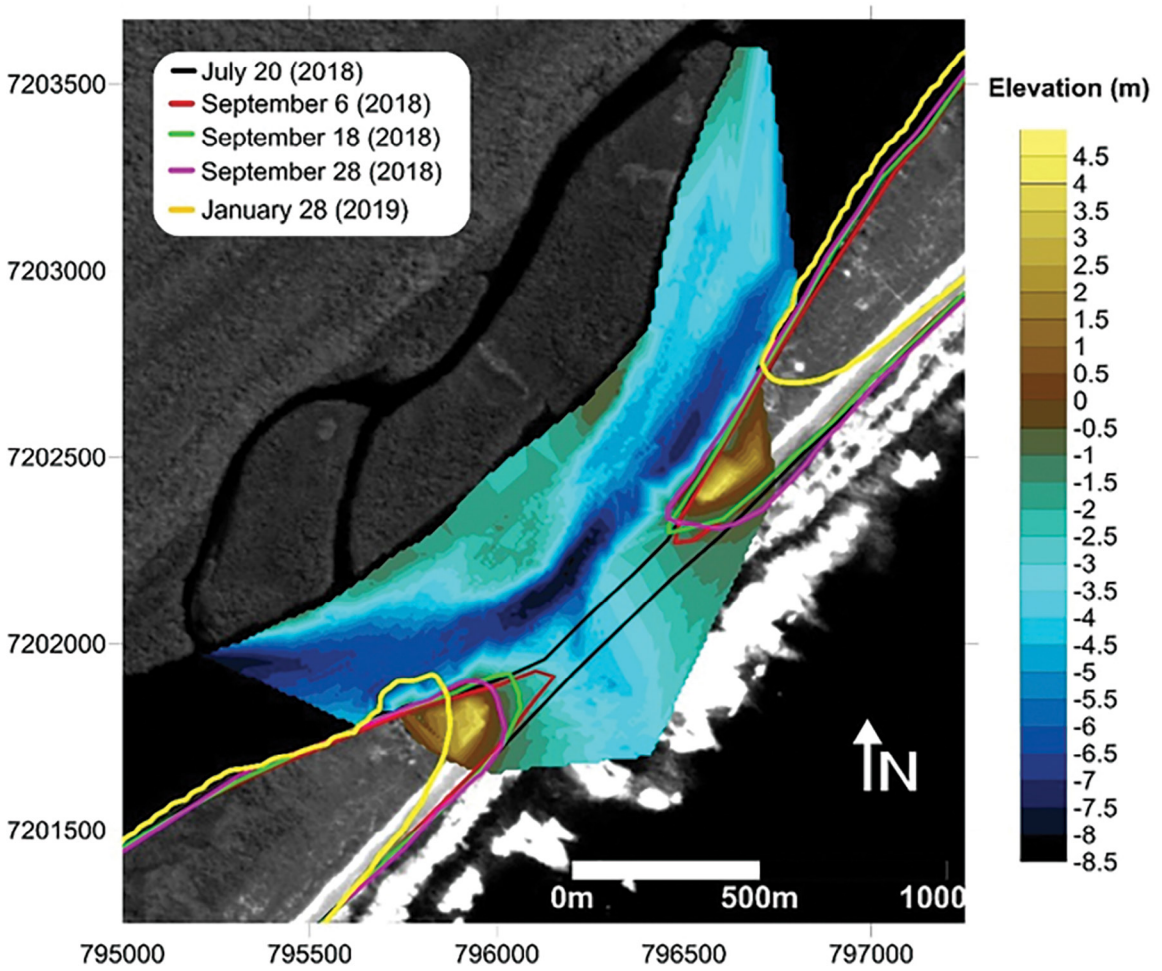

Figure 12. Coastline evolution around the new Ararapira inlet based on satellite images (July 2018 to January 2019) and surveyed bathymetry (September 2018) of the new channel.

new inlet reaches its equilibrium, as discussed in other cases of inlet openings (e.g., Liu et al., 1993). The water exchange between the estuary and ocean became more efficient through the new inlet, leading to its fast widening. In contrast, the old inlet currently presents growing sandbars, indicating its gradual narrowing (Fig. 13).

As expected, (e.g., FitzGerald et al., 2001), after the opening of the new inlet and its dominance in water exchange, the old inlet has a decreased flow intensity through its channel, allowing an increased bypass of sediments transported by the longshore drift, leading to the deposition of the material inside the channel. The gradual abandonment of the old inlet leads to its shoaling, and, as summarized in Pope (2000), double inlet systems are not stable, and one inlet tends to close. Thereby, an increased volume of sediment reaches the new inlet southern margin, which becomes partially trapped due to the new inlet's hydraulic jetty effect. This process may have favored the stability of this margin and facilitated the process of erosion at the northern margin, due to the lack of available sediments at the northern margin of the new inlet, which is the downdrift portion of the new system when considering the net northward longshore drift in the region. Additionally, longshore moving sediments that reach the channels are partially diverted landwards by tidal flows through the main channels, forming the flood tidal shoals, as seen in Figure 13. Waves probably aid the influx of littoral sediments into the lagoon. It is evident from the accretion on the inner shore south of the

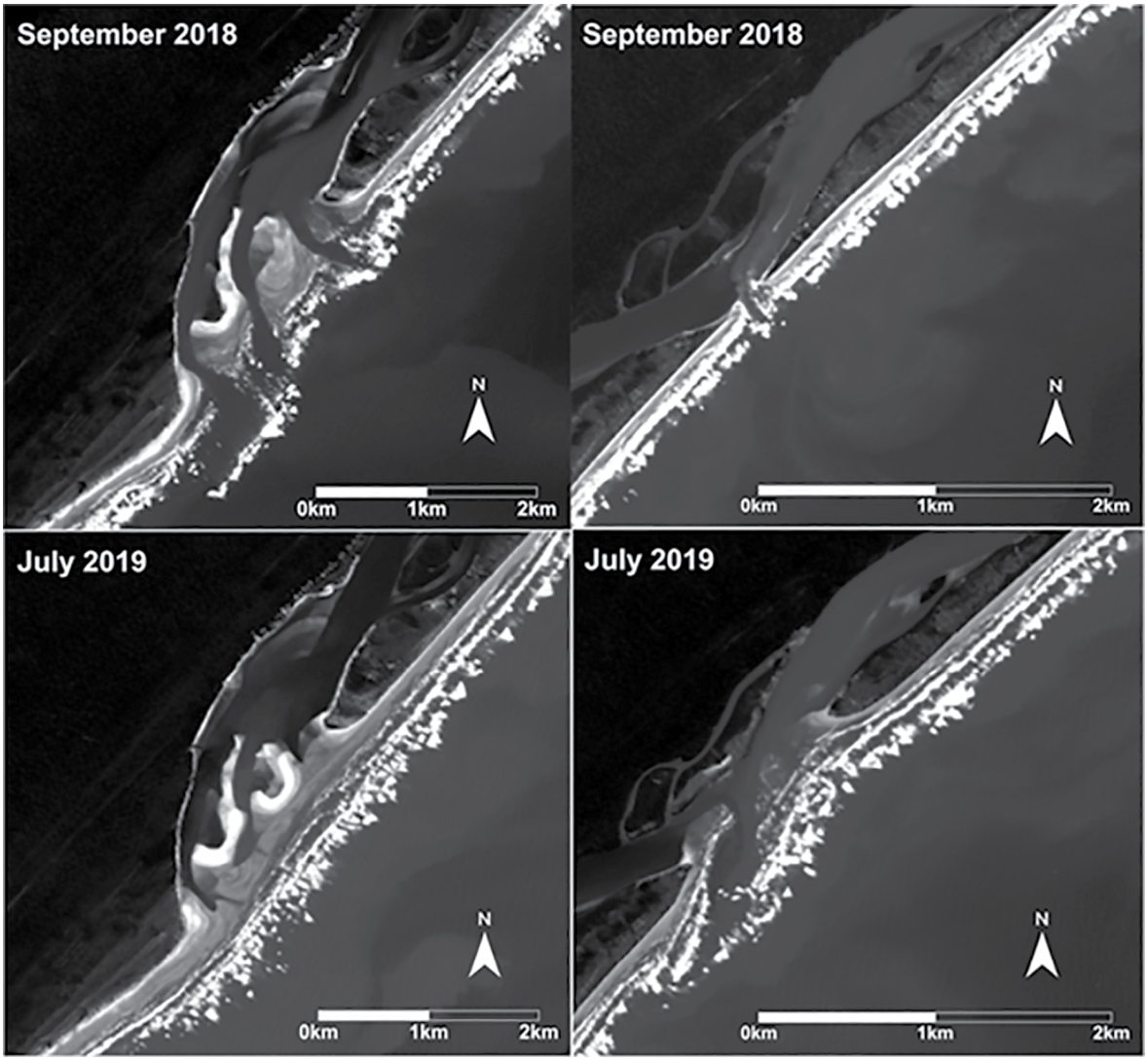

Figure 13. Images of the old Ararapira inlet (left) and new inlet (right) in September 2018 and in July 2019 (Images: Landsat 8).

main channel bend, as observed in Figure 12 (yellow shoreline).

This study has been a valuable opportunity to assess the morphological evolution of an inlet system and the opening of a new inlet through the breaching of a narrow barrier. Only rare occasions allow the monitoring of the early morphological evolution of newly opened inlets through natural processes (e.g., Liu et al., 1993; FitzGerald and Pendleton, 2002) or artificial openings (e.g., Kana and Mason, 1998; Cleary and FitzGerald, 2003; Erickson et al., 2003; Vila-Concejo et al., 2003; Vila-Concejo et al., 2004), providing relevant background information for the management of such areas. Morphological changes at the entrance of coastal water bodies have several environmental implications, such as propagation of tides that generate co-oscillations in the estuaries, controlling variations of estuarine water volume, mixing, and water renewal rate (Dyer, 1997). Changes in inlet morphology also cause changes in estuarine processes (Aldridge, 1997; Friedrichs and Aubrey, 1988; Hinrichs et al., 2018; Siegle et al., 2019) with an essential role of tidal asymmetry in the residual sediment transport and morphological evolution of estuaries (Dronkers, 1986). The resilience of estuaries is also dependent on the residence time of water within the system (Wolanski et al., 2004), which is expected to change with morphological changes at its inlets.

The scenarios of climate change and sea-level rise tend to make such barrier breaches more frequent in the next decades; therefore, understanding their evolution and impacts on the adjacent estuaries and beaches is of prime importance.

CONCLUSIONS

Combining the analysis of the morphological evolution of a subtropical barrier inlet system at different time scales, we assessed: i. the long-term inlet morphological changes and its updrift migration; and ii. the opening of a new inlet and its early stages of evolution. The analysis of the coastline variation through the Landsat multispectral images corroborated observations and predictions made in previous studies. The updrift migration of the old inlet with a continuous erosion process at the inner portion of the southern margin of the inlet and an accretion process are intercalated with some erosive events, at its northern margin. The erosion/accretion process is almost continuous until August 2018, and a new entrance is formed through the barrier break approximately 6 km north of the old entrance. Once open, the inlet quickly becomes the main connection for the system's water exchange, reaching a width of approximately 1,370 m in March 2019. The decreasing widening rates of the channel, from 16 to 2.8 m per day, indicates that it is reaching its equilibrium width. Water exchange occurring mainly through the new channel, makes the old inlet flows weaker, resulting in shoaling and gradual infilling of the old inlet, resulting in increased sediment bypass. Although precocious to assessing the migration pattern of the newly formed inlet, the first stages of shoreline evolution show the continuing updrift migration (southwards), a similar pattern to the old inlet. This tendency is probably related to the inner channel shore-parallel orientation, directing the main flow southwards.

In this study, we provide a first assessment of the new Ararapira inlet evolution, indicating the need for further studies of its evolution and the changes induced in its estuarine and coastal systems. Such knowledge is of prime importance for the correct management and evolutionary prediction of such systems.

ACKNOWLEDGMENTS

Members of the LOCG-CEM-UFPR, LDC- IOUSP, technical team, Alexandre Bernardino Lopes (topography, geodesy and cartography laboratory – CEM), residents of local communities, and friends who participated in the data collection effort. This study was financed in part by the Coordenação de Aperfeiçoamento de Pessoal de Nível Superior - Brasil (CAPES) - Finance Code 001. Diana Italiani received a CAPES Ph.D. scholarship. Eduardo Siegle is a CNPq research fellow.

AUTHOR CONTRIBUTIONS

D.M.I.: Conceptualization; Investigation; Formal Analysis; Methodology; Writing – original draft; Writing – review & editing; E.S.: Conceptualization; Investigation; Methodology; Supervision; Funding acquisition; Writing – review & editing; M.A.N.: Conceptualization; Investigation; Methodology; Supervision; Funding acquisition; Writing – review & editing.

REFERENCES

Aldridge, J. N. 1997. Hydrodynamic model predictions of tidal asymmetry and observed sediment transport paths in Morecambe Bay. *Estuarine, Coastal and Shelf Science*, 44, 39-56.

Alesheikh, A. A., Ghorbanali, A. & Nouri, N. 2007. Coastline change detection using remote sensing. *International Journal of Environmental Science and Technology*, 4(1), 61-66.

Ambrosio, B. G., Sousa, P. H. G. O, Gagliardi, M. H. & Siegle, E. 2020. Wave energy distribution at inlet channel margins as a function of ebb tidal delta morphology: Cananéia Inlet, São Paulo, Brazil. *Anais da Academia Brasileira de Ciências*, 92(1), e20180677. DOI https://doi.org/10.1590/0001-3765202020180677

Angulo R. J. 1993. Variações na configuração da linha de costa no Paraná nas últimas quatro décadas. *Boletim Paranaense de Geociências*, 41, 52-72.

Angulo R. J. 1999. Morphological characterization of the tidal deltas on the coast of the State of Paraná. *Anais da Academia Brasileira de Ciências,* 71(4), 935-959.

Angulo R. J., Souza M. C. & Müller M. E. 2009. Previsão e consequências da abertura de uma nova barra no Mar do Ararapira, Paraná-São Paulo, Brasil. *Quaternary and Environmental Geosciences*, 1(2), 67-75.

Angulo, R. J., Souza, M. C. & Müller, M. E. 2007. *Evolução do esporão e conseqüências da abertura de uma nova desembocadura do Mar do Ararapira (Paraná - Brasil),* Congresso da Associação Brasileira de Estudos do Quaternário (ABEQUA), 4-11 November, Belém, PA, ABEQUA.

Aubrey, D. G. & Speer, P. E. 1984. Updrift migration of tidal inlets. *Journal of Geology*, 92, 531-545.

Bazzo, J. 2011. The weave of kinship and the ever-mobile fishing village of Barra de Ararapira (Superagüi Island, Guaraqueçaba, Paraná, Brazil). *Vibrant: Virtual Brazilian Anthropology*, 8(2), 164-196. DOI: https://doi.org/10.1590/S1809-43412011000200008

Cassiano, G. F. & Siegle, E. 2010. Migração lateral da desembocadura do Rio Itapocú, SC, Brasil: evolução morfológica e condicionantes físicas. *Revista Brasileira de Geofísica*, 28(4), 537-549. DOI: https://doi.org/10.1590/S0102-261X2010000400001

Cleary, W. J. & Fitzgerald, D. M. 2003. Tidal inlet response to natural sedimentation processes and dredging-induced tidal prism changes: Mason inlet, North Carolina. *Journal of Coastal Research*, 19(4), 1018-1025.

Cussioli, M. C., Siegle, E., Miranda, L. B. & Schettini, C. A. F. 2011. Morphodynamics at the Itanhém Inlet. *The Proceedings of the Coastal Sediments*, 11, 380-391.

Davis Junior, R. A. & Fitzgerald, D. M. 2004. *Beaches and coasts*. New Jersey: Blackwell Publishing.

Dean, R. G. & Dalrymple, R. A. 2002. *Coastal processes with engineering applications*. New York: Cambridge University Press.

Dronkers, J. 1986. Tidal asymmetry and estuarine morphology. *Netherlands Journal of Sea Research*, 20(2-3), 117-131.

Dyer, K. R. 1986. *Coastal and estuarine sediment dynamics*. New Jersey: John Wiley & Sons.

Erickson, K. M., Kraus, N. C. & Carr, E. E. 2003. *Circulation change and ebb shoal development following relocation of Mason Inlet, North Carolina*, CD-ROM. The Proceedings of Coastal Sediments, Sand Key, F.L.

Escoffier, F. F. 1940. The stability of tidal inlets. *Shore & Beach*, 8(4), 114-115.

Ferreira, A. T. S., Amaro, V. E. & Santos, M. S. T. 2014. Geodésia aplicada à integração de dados topográficos e batimétricos na caracterização de superfícies de praia. *Revista Brasileira de Cartografia*, 66(1), 167-184.

FitzGerald, D.M. 1988. Shoreline erosional-depositional processes associated with tidal inlets. In: Mehta, A.J. (ed.). Estuarine Cohesive Sediment Dynamics. Lecture Notes on Coastal Estuarine Studies. pp. 186-225.

Fitzgerald, D. M., Kraus, N. C. & Hands, E. B. 2001. *"Natural mechanisms of sediment bypassing at tidal inlets," Coastal Engineering Technical Note CHETN-IV-30.* U.S. Army Engineer Research and Development Center, Vicksburg, M.S.

Fitzgerald, D. M. & Pendleton, E. 2002. Inlet formation and evolution of the sediment bypassing system: new inlet, Cape Cod, Massachusetts. *Journal of Coastal Research*, 36(spe1), 290-299. DOI: https://doi.org/10.2112/1551-5036-36.sp1.290

Friedrichs, C. T. & Aubrey, D. G. 1988. Non-linear tidal distortions in shallow well-mixed estuaries: a synthesis. *Estuarine, Coastal and Shelf Sciences*, 27, 521-545.

Guedes, C. C. F., Giannini, P. C. F., Sawakuchi, A. O., Dewitt, R., Nascimento Junior, D. R., Aguiar, V. A. P. & Rossi, M. G. 2011. Determination of controls on Holocene barrier progradation through application of OSL dating: the Ilha Comprida Barrier example, Southeastern Brazil. *Marine Geology*, 285(1-4), 1-16.

Harari, J. & Camargo, R. 1994. Simulação da propagação das nove principais componentes de maré na plataforma sudeste brasileira através de modelo numérico hidrodinâmico. *Boletim do Instituto Oceanográfico*, 42(1-2), 35-54.

Hayes, M.O. 1979. Barrier island morphology as a function of tidal and wave regime. In: Leatherman, S. P. (ed.). *Barrier Islands*. New York, U.S.: Academic Press.

Hayes, M. O. & Fitzgerald, D. M. 2013. Origin, evolution, and classification of tidal Inlets. *Journal of Coastal Research*, 69, 14-33.

Hinrichs, C., Flagg, C. N. & Wilson, R. E. 2018. Great South Bay after sandy: changes in circulation and flushing due to new inlet. *Estuaries and Coasts*, 41, 2172-2190. DOI: https://doi.org/10.1007/s12237-018-0423-6

IBGE (Instituto Brasileiro de Geografia e Estatística). 2017. *Homepage*. Brasília, Brazil: IBGE. Available at: http://www.ibge.gov.br [27 Apr. 2017].

Italiani, D. M. 2019. *Morfodinâmica da desembocadura do Ararapira SP/PR: evolução, forçantes e previsões*. PhD, Federal University of Paraná, Paraná.

Kana, T. W. & Mason, J. E. 1988. Evolution of an ebb-tidal delta after an inlet relocation. *Lecture Notes on Coastal and Estuarine Studies*, 29, 382-409.

Komar, P. D. 1996. Tidal-inlet processes and morphology related to the transport of sediments. *Journal of Coastal Research*, 1(spe23), 23-45.

Komar, P. D. 1998. *Beach processes and sedimentation*. 2nd ed. Englewood Cliffs, N. J.: Prentice Hall.

Kumpera, B. 2007. *Contribuição ao processo sedimentar atual no Canal do Ararapira, sistema-estuarino-lagunar de Cananéia--Iguape (SP).* MSc, University of São Paulo, São Paulo.

Liu, J. T., Stauble, D. K., Giese, G. S. & Aubrey, D. G. 1993. Morphodynamic evolution of a newly formed tidal inlet. In: Aubrey, D. J. & Giese, G. S. (eds.). *Formation and evolution of multiple tidal inlets*. New Jersey, U.S.: John Wiley & Sons.

Marone, E. & Camargo, R. 1995. Efeitos da maré meteorológica na baía de Paranaguá, PR. *Nerítica*, 8, 71-81.

McFeeters, S. K. 1996. Using the normalized difference water index (NDWI) within a geographic information system to detect swimming pools for mosquito abatement: a practical approach. *Remote Sensing*, 5(7), 3544-3561.

Mihály, P. & Angulo, R. J. 2002. Dinâmica da desembocadura do corpo lagunar do Ararapira. *Revista Brasileira de Geociências*, 32, 217-222.

Moreira, S., Freitas, M. C., Andrade, C. & Bertin, X. 2019. Processes controlling morphodynamics of artificially breached barriers. *Estuarine, Coastal and Shelf Science*, 225, 106231.

Müller, M. E. J. 2010. Estabilidade morfo-sedimentar do Mar do Ararapira e conseqüências da abertura de uma nova barra. MSc, Federal University of Paraná, Paraná.

Nemes, D. D. & Marone, E. 2010. Caracterização das ondas de superfície na plataforma interna do estado do paraná. *Boletim Paranaense de Geociências*, 68-69, 20-22.

Nimer, E. 1989. *Climatologia do Brasil*. Rio de Janeiro, Brazil: IBGE, Série Recursos Naturais e Meio Ambiente.

O'Brien, M. P. 1969. Equilibrium flow areas of inlets on sandy coasts. *Journal of Waterways, Harbors and Coastal Engineering Division*, 95(1), 43-52.

Pianca, C., Mazzini, P. L. F. & Siegle, E. 2010. Brazilian offshore wave climate based on NWW3 reanalysis. *Brazilian Journal of Oceanography*, 58(1), 53-70.

Pope, J. 2000. *"Where and why channels shoal: a conceptual geomorphic framework," ERDC/CHL CHETN-IV-12.* U.S. Army Engineer Research and Development Center, Vicksburg, M.S.

PORTOBRÁS - Empresa de Portos do Brasil S.A. 1988. *Relatório de apresentação das medições meteorológicas observadas em Pontal do Sul, Paranaguá-PR, período set.1982 a dez. 1986*. Rio de Janeiro, Brazil: INPH.

PORTOBRÁS - Empresa de Portos do Brasil S.A. 1983. *Campanha de medições de ondas em Paranaguá-PR, período 21.08.1982 a 21.01.1983*. Rio de Janeiro, Brazil: INPH.

Reef, K. R. G., Roos, P. C., Andringa, T. E., Dastgheib, A. & Hulscher, S. J. M. H. 2020. The impact of storm-induced breaches on barrier coast systems subject to climate change—a stochastic modelling study. *Journal of Marine Science and Engineering,* 8(4), 271. DOI: https://doi.org/10.3390/jmse8040271

Rocha R. P., Sugahara, S. & Silveira, R. B. 2004. Sea waves generated by extratropical cyclones in the South Atlantic Ocean: hindcast and validation against altimeter data. *Weather and Forecasting*, 19(2), 398-410.

Safak, I., Warner, J. C. & List, J. H. 2016. Barrier island breach evolution: alongshore transport and bay-ocean pressure gradient interactions. *Journal of Geophysical Research: Oceans*, 121(12), 8720-8730. DOI: https://doi.org/10.1002/2016JC012029

Siegle, E. & Asp, N. E. 2007. Wave refraction and longshore transport patterns along the southern Santa Catarina coast. *Brazilian Journal of Oceanography*, 55(2), 109-120.

Siegle, E., Couceiro, M. A. A., Sousa, S. H. M., Figueira, R. C. L. & Schettini, C. A. F. 2019. Shoreline retraction and the opening of a new inlet: implications on estuarine processes. *Estuaries and Coasts*, 42, 2004-2019. DOI: https://doi.org/10.1007/s12237-019-00635-w

Silva, F. G., Sousa, P. H. G. O & Siegle, E. 2016. Longshore transport gradients and erosion processes along the Ilha Comprida (Brazil) beach system. *Ocean Dynamics*, 66(6-7), 853-865. DOI: https://doi.org/10.1007/s10236-016-0956-9

Souza, M. C. 1999. *Mapeamento da planície costeira e morfologia e dinâmica das praias do município de Itapoá, Estado de Santa Catarina: subsídios à ocupação*. MSc, Federal University of Paraná, Paraná.

Tessler, M. G. & Mahiques, M. M. 1993. Utilization of coastal geomorphic features as indicators of longshore transport: examples of the southern coastal region of the State of São Paulo, Brasil. *Journal of Coastal Research*, 9, 823-830.

Tessler, M. G. 1988. *Dinâmica sedimentar quaternária no litoral sul paulista*. PhD, University of São Paulo, São Paulo.

Tessler, M. G. & Goya, S. C. 2005. Processos costeiros condicionantes do litoral brasileiro. *Revista do Departamento de Geografia*, 17, 11-23.

Trenhaile, A. S. 1997. *Coastal dynamics and landforms*. New York, U.S.: Oxford University Press.

Trombetta, T. B., Oleinik, P. H., Guimarães, R. C., Kirinus, E. D. P., Marques, W. C. & Isoldi, L. A. 2018. Longshore sediment transport on the Brazilian continental shelf. *Scientia Plena*, 15.

van de Kreeke, J. 1992. Stability of tidal inlets; Escoffier's analysis. *Shore & Beach*, 60, 9-12.

Vila-Concejo, A., Ferreira, Ó., Matias, A. & Dias, J. M. A. 2003. The first two years of an inlet: sedimentary dynamics. *Continental Shelf Research*, 23(14-15), 1425-1445.

Vila-Concejo, A., Ferreira, Ó., Morris, B. D., Matias, A. & Dias, J. M. A. 2004. Lessons from inlet relocation: examples from Southern Portugal. *Coastal Engineering*, 51(10), 967-990.

Wolanski, E., Boorman, L. A., Chícharo, L., Langlois-Salious, E., Lara, R., Plater, A. J., Uncles, R. J. & Zalewski, M. 2004. Ecohydrology as a new tool for sustainable management of estuaries and coastal waters. *Wetlands Ecology and Management,* 12(4), 235-276.